A CURRENT FED TWO-INDUCTOR BOOST CONVERTER FOR GRID INTERACTIVE PHOTOVOLTAIC APPLICATIONS

Quan Li and Peter Wolfs

Central Queensland University

Abstract

A current fed two-inductor boost converter is combined with a low frequency unfolder stage to produce a Module Integrated Converter (MIC) for photovoltaic applications. A two-phase buck converter with an interphase transformer is modulated to produce a rectified sinusoid waveform as an input to the fixed duty cycle two-inductor boost cell. The boost cell features an integrated magnetics approach to combine the two inductors and the transformer cores, non-dissipative snubbers to recover switching losses and silicon carbide output rectifiers. The MIC interfaces with the mains via an unfolder stage which uses optically driven mosfets as switching elements. Experimental results for a converter with an average power of 50 W are provided.

1. INTRODUCTION

Module Integrated Converters (MICs), with rated powers below 500 W, have become one of the main streams in the PV market, [1]. MIC technology employs the building block concept which integrates the grid-connectable power converter to the PV module and caters better to the goal of minimizing the cost and maximizing the efficiency of the PV system. Amongst a variety of converter topologies, the two-inductor boost converter, together with a DC-AC inverter, shown in Figure 1, has been proved to be one of the favourable candidates for MICs in the grid interactive photovoltaic applications, [2].

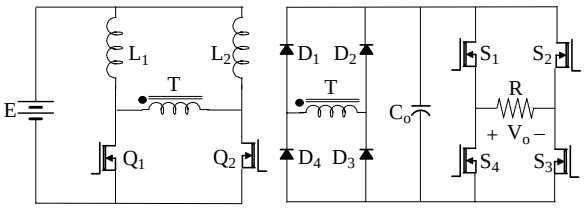

Figure 1. The Two-Inductor Boost Converter with an Inverter

In Figure 1, the high frequency transformer isolated two-inductor converter generates a fixed DC link. The inverter produces an AC current for injection into the grid. As the input voltage for the DC-AC inverter is fixed, the Pulse-Width Modulation (PWM) is commonly used to produce acceptable sinusoidal waveforms. However, the PWM control technique requires a relatively complex circuit to implement and introduces additional switching loss.

This paper proposes a current fed two-inductor boost converter which is able to generate rectified sinusoidal waveforms on the DC link. This significantly simplifies the design of the DC-AC inverter and reduces the inverter to an unfolder. The proposed topology is shown in Figure 2. The front-end two-phase buck converter acts as the current source and it is interfaced with the two-inductor boost converter through an auto transformer. The rectification stage employs a voltage doubler instead of the full bridge diode rectifier as shown in Figure 1.

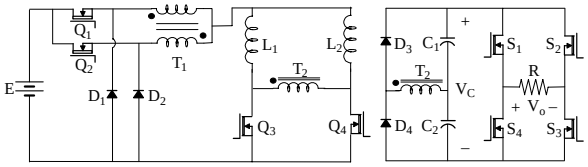

Figure 2. The Current Fed Two-Inductor Boost Converter with an Unfolder

The paper studies in detail the operation of the three individual stages of the converter including the buck stage, the boost stage and the inversion stage. Experimental results of a 50 W converter with 20 V input and 240 V RMS output are provided.

2. THE TWO-PHASE BUCK CONVERTER

The hard-switched two-inductor boost converter can produce a variable output voltage by varying the switching duty ratios. Because the inductors act as the current sources, they require that at least one switch be closed. This results in a minimum switch duty ratio of 50% and the minimum output voltage will be higher than twice the input voltage. Zero output voltage cannot be reached. A buck converter must be placed before the boost-derived two-inductor converter to achieve a zero output voltage. In Figure 2, a two-phase buck converter is used to obtain the advantages brought by higher equivalent switching frequencies without suffering higher switching losses in the buck converter mosfets.

Multi-phase converter arrangements have recently been widely adopted as an efficient approach to parallel multiple converters to provide high current output, [3]. Under multi-phase operation, the currents with an equal phase shift, which is the quotient of 360° divided by the number of phases, are added

together and the equivalent input and output ripple current frequency will be multiplied by the number of the phases. The converter also has less input or output current ripple as those in each phase cancel, [4].

The topology shown in Figure 2 can be further improved by using synchronous rectifiers as shown in Figure 3. Although the simulation results of the lateral thin-film Schottky rectifier with the forward voltage drop as low as 0.27 V have been recently published, [5], the lowest diode forward voltage drop most available is around 0.5 V and its further reduction presents a great challenge, [6]. In the synchronous rectifier, the diode is replaced by the mosfet. This design is able to largely improve the converter efficiency, as the forward resistance of the synchronous mosfet can be very low, [7]. Dead time must be applied to prevent "shoot-through". A Schottky diode is placed in reverse parallel with the synchronous mosfet to avoid the load current flowing through the body diode, which normally has a higher voltage drop and inferior reverse recovery.

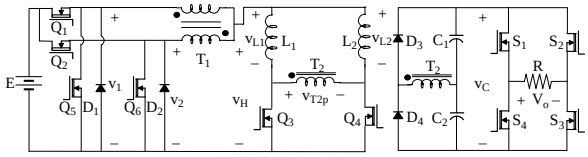

Figure 3. The Converter with the Synchronous Buck Converters

The output of the two-phase synchronous buck rectifier is fed to the two-inductor boost converter through an interphase transformer (IPT), with 1:1 turns ratio. The ITP is a tapped inductor, which is widely used in mains frequency high pulse number rectifiers, [8], but only occasionally found in DC-DC converter applications, [9]. The advantage of employing an ITP is that the equivalent switching frequency is doubled and the three-level modulation is achieved at the output. This topology requires good current sharing between the phases to avoid ITP saturation. Current mode control is a suitable solution.

3. THE TWO-INDUCTOR BOOST CONVERTER

Magnetic integration, which merges the discrete transformers and inductors into a single core configuration, assists in reducing the size of the switched mode power converters, [10]. In the converter shown in Figure 3, the KVL gives:

$$v_{T2p} = v_{L2} - v_{L1} \qquad (1)$$

where v_{T2p}, v_{L2} and v_{L1} are respectively the voltages across the transformer T_2 primary, the inductors L_2 and L_1. Therefore the fluxes in the two inductors L_1, L_2 and the transformer T_2 primary are linearly related as shown in Equation (2) and this allows the magnetic integration to be carried out:

$$N_{p2} \cdot \Delta\phi_{T2} = N_{L2} \cdot \Delta\phi_{L2} - N_{L1} \cdot \Delta\phi_{L1} \qquad (2)$$

where N_{p2} and $\Delta\phi_{T2}$ are respectively the number of primary turns and the change in flux in the transformer T_2; N_{L2} and $\Delta\phi_{L2}$ are the number of turns and the change in flux in the inductor L_2 and N_{L1} and $\Delta\phi_{L1}$ are the number of turns and the change in flux in the inductor L_1. If $N_{p2} = N_{L1} = N_{L2}$, Equation (2) can be simplified to:

$$\Delta\phi_{T2} = \Delta\phi_{L2} - \Delta\phi_{L1} \qquad (3)$$

Three cores for the two inductors and the transformer can be integrated if a three-leg core structure is selected and the winding arrangements are such that the relationship between the individual fluxes given in Equation 3 is fulfilled. A Ferroxcube ETD core with equal air gaps in both of the two outer legs is used. A top-view diagram of the core and winding construction is given in Figure 4. The windings between terminals 1 and 2 form inductor L_1, those between terminals 1 and 3 form inductor L_2, those between terminals 2 and 3 form transformer T_2 primary and those between terminals 4 and 5 form transformer secondary. The transformer primary and the two inductors have the same number of turns.

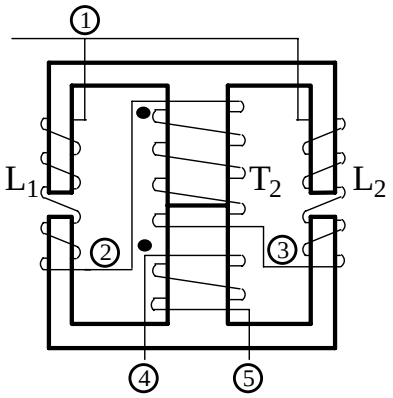

Figure 4. Top-View of the Integrated Inductors and Transformer

In the operation of the hard-switched two-inductor boost converter, a low transformer leakage inductance is a must. Otherwise the energy stored in the leakage inductance will cause higher switch voltage at mosfet turn-off, [11]. Various voltage clamping or snubber circuits have been developed to control the peak switch voltage. Non-dissipative snubbers, which are able to improve the converter efficiency, are of special interest, [12]. The non-dissipative snubber has been previously introduced with the two-inductor boost converter, [13]. At switch turn off, the transformer

leakage inductance energy is transferred losslessly back to the supply through the snubber capacitors and inductor. However, this snubber circuit uses separate inductors for individual mosfets. Figure 5 shows the converter with a variation of the non-dissipative snubber. Only one snubber inductor is used and the current return path is shared by the turn-on of the two mosfets. Instead of the diode in series with the snubber inductor, a diode pair D_{sr1} and D_{sr2}, with common anode, must be used to prevent the current from flowing between the two snubber capacitors C_{s1} and C_{s2}. As the input voltage of the two-inductor boost converter varies, the snubber circuit only becomes active when the snubber capacitor is charged higher than E during the mosfet turn-off.

The rectification stage of the two-inductor boost converter is implemented with a voltage doubler. Normal PN junction diodes present a relatively long reverse recovery time. This reduces the converter efficiency and may even lead to thermal run-away of the diodes. Recently, SiC Schottky diodes have been developed and they have high reverse breakdown voltage ratings and near-zero reverse recovery time, [14]. SiC Schottky diodes are especially suited in this converter application.

The two-inductor boost converter produces a rectified sinusoid to simplify the DC-AC inverter design. If the input voltage of the converter is E, the duty ratio of the buck stage mosfets Q_1 and Q_2 is D_{buck} and that of the boost stage mosfets Q_3 and Q_4 is D_{boost}, the output voltage of the two-inductor boost converter can be obtained as:

$$V_C = \frac{2D_{buck}}{1 - D_{boost}} n_{T2} E \qquad (4)$$

where n_{T2} is the turns ratio of the transformer T_2. In order to produce sinusoidal output, D_{boost} can be a fixed value, which is slightly greater than 50%, and D_{buck} is required to be modulated in a sinusoidal manner.

4. THE UNFOLDER

As the input of the DC-AC inverter is the rectified sinusoidal waveform, the control for the inversion stage is relatively simple – the square-wave control can be applied. The output waveform of the unfolder is sinusoidal and can be directly applied to the grid. In the unfolder operation, the switches turn on and off under grid frequency and this avoids high switching losses under the PWM control.

Electrically isolated optical mosfet drivers are used to provide the gate signals. The output current of the optical mosfet drivers must be relatively big to achieve short turn-on transitions. The optical mosfet drivers must also have an embedded active discharge circuit to discharge the mosfet gate capacitance to obtain fast turn-off behaviours.

5. THE THEORETICAL AND THE EXPERIMENTAL RESULTS

The switching frequency of the buck stage mosfets f_{buck} and that of the boost stage mosfets f_{boost} are respectively selected to be $f_{buck} = 150\,kHz$ and $f_{boost} = 75\,kHz$. The theoretical waveforms of the converter with above parameters over high frequency cycles are given in Figure 6. Figures 6(a) and (b) respectively shows the converter waveforms when $D_{buck} < 50\%$ and $D_{buck} > 50\%$. The voltage after the ITP swings between zero and half of the input voltage when D_{buck} is lower than 50%, while it swings between half of the input voltage and the full input voltage when D_{buck} is greater than 50%. The three levels and the frequency doubling effect can be seen in V_H waveform in both cases. The main components are:

- Two-phase synchronous step-down switching regulator – Linear Technology LTC1929CG; current transformers are used for current sensing;
- Synchronous rectifier mosfet – International Rectifier IRF7901D1, dual mosfet plus Schottky diode, $V_{DS} = 30\ V$, $I_D = 6.2\ A$, $V_{F,Schottky} = 0.58\ V$, $R_{DS(on),control} = 0.038\ \Omega$, $R_{DS(on),synchronous} = 0.032\ \Omega$;
- Interphase transformer – Core type Epcos EFD15, ferrite grade N87, 0.15 mm air gap, 7 turns plus 7 turns;
- Inductors L_1 and L_2, 23 turns, and transformer T_2 23 to 98 turns – Core type Ferroxube ETD39 with 0.5 mm air gap in the two outer legs, ferrite grade 3F3;
- Two-inductor boost converter mosfet – Fairchild FQB50N06, $V_{DS} = 60\ V$, $I_D = 50\ A$, $R_{DS(on)} = 0.022\ \Omega$;
- Snubber capacitor – Kemet class X7R surface mount capacitor C0805C104K5RAC, $C = 0.1\ \mu F$, $V_{dc} = 50\ V$;
- Snubber inductor – 10 Epcos 100 μH axial Large Bobbin Core (LBC) series inductors in parallel, $Q = 50$ under 796 kHz;
- Snubber Schottky diode – Fairchild SS26, $I_F = 2.0\ A$, $V_{RRM} = 60\ V$, $V_F = 0.7\ V$;
- Rectifier Schottky diode – Microsemi UPSC600, $I_F = 1.0\ A$, $V_{RRM} = 600\ V$, $V_F = 1.6\ V$;

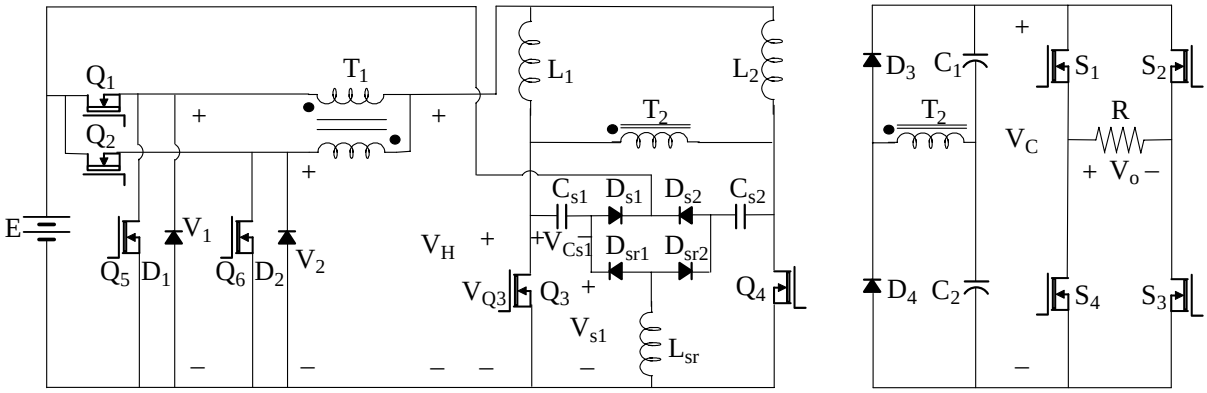

Figure 5. The Converter with the Non-Dissipative Snubber

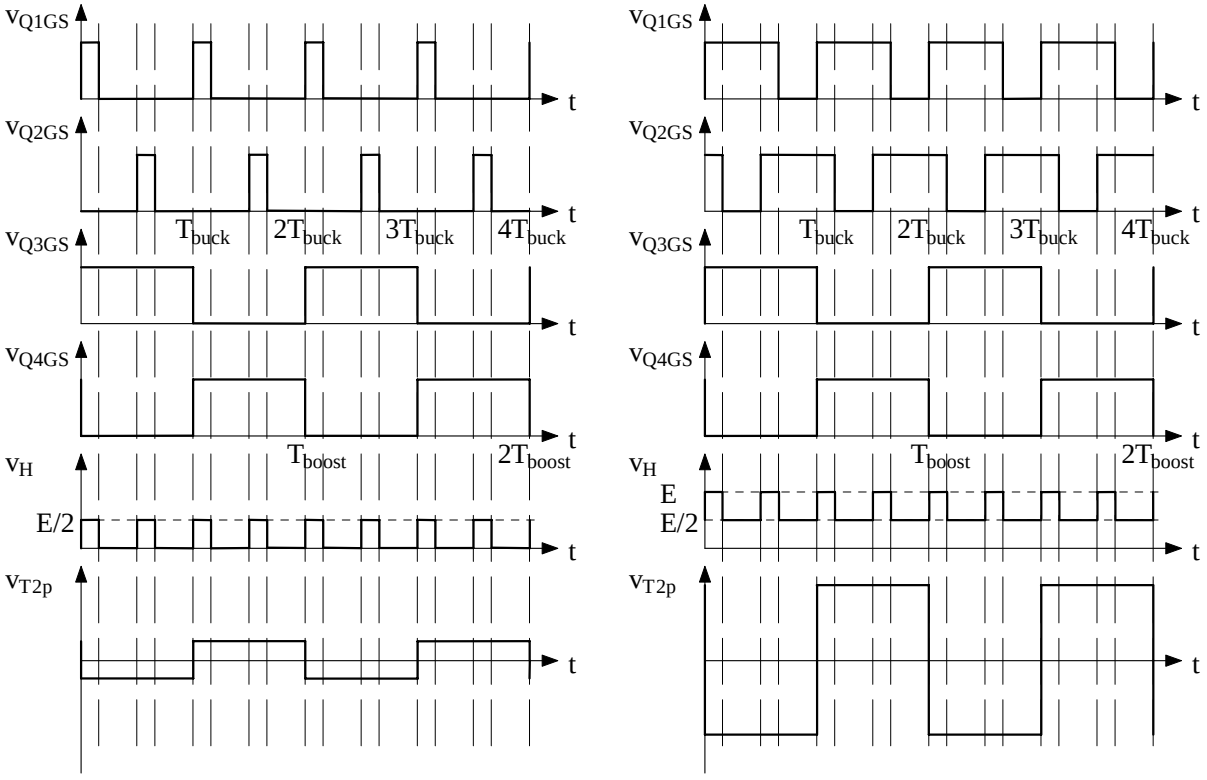

(a) (b)

Figure 6. Theoretical Waveforms (a) D_{buck} < 50% (b) D_{buck} > 50%

- Rectifier capacitor – 2 pairs of 4 parallel connected Phycomp class X7R multilayer ceramic surface mount capacitor, $C = 0.022\ \mu F$, $V_{dc} = 200\ V$;
- Unfolder mosfet – International Rectifier IRF830AS, $V_{DS} = 500\ V$, $I_D = 5.0\ A$, $R_{DS(on)} = 1.4\ \Omega$;
- Unfolder photovoltaic mosfet driver – Dionics DIG-11-15-30-DD, output open circuit voltage $V_{oc} = 15\ V$ and short circuit current $I_{sc} = 60\ \mu A$ at input current $I_{led} = 30\ mA$ with 50% duty cycle, isolation voltage $V_{iso} = 2500\ V$.

Figures 7 to 11 show the experimental waveforms. The waveforms under static tests showing the frequency doubling effect of the two-phase synchronous buck converter through the ITP are given in Figure 7. From top to bottom, Figures 7(a) and (b) respectively shows the waveforms of V_1, V_2 and V_H with duty ratio D_{buck} lower and greater than 50%. The voltage after the ITP swings between 0 V and 10 V when D_{buck} is lower than 50%, while it swings between 10 V and 20 V when D_{buck} is greater than 50%. In either case, the frequency of the voltage V_H after the ITP is twice that of voltage V_1 or V_2 before. Figure 8 shows the two-inductor boost converter output V_C and the input V_H from top to bottom during

sinusoidal modulation. High frequency switching is absent in V_H due to oscilloscope aliasing. Figure 9 shows the gate waveforms of the low frequency unfolder switches S_2 (S_4), S_1 (S_3) and the output voltage V_O from top to bottom. Figure 10 shows the mosfets Q_3, Q_4 drain source voltages and voltage across the SiC Schottky diode when the converter output voltage is close to its peak. With the lossless snubber, the voltage stress across the mosfets is controlled within 60 V whereas peak switch voltage higher than 100 V had been seen before the snubber circuit was put in. The voltage waveform across the diode is clean, without any over voltage due to reverse recovery.

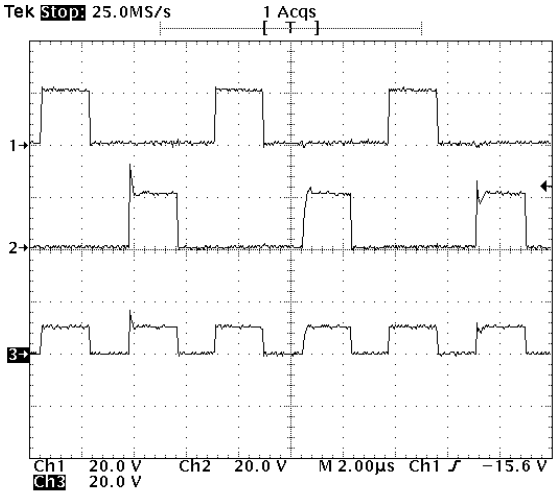

(a)

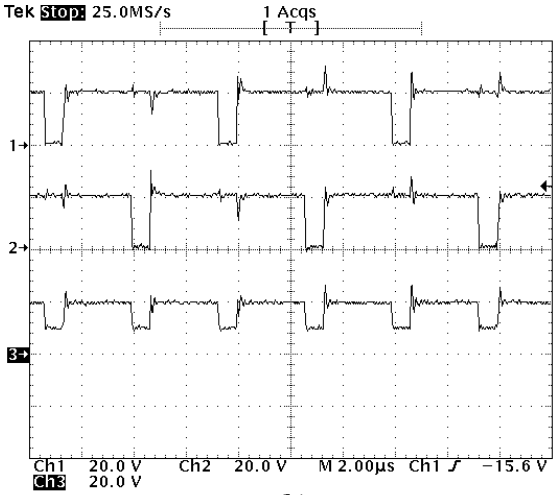

(b)

Figure 7. Two-Phase Synchronous Buck Converter Waveforms (a) $D_{buck} < 50\%$ (b) $D_{buck} > 50\%$

Figure 11 shows the mosfet Q_3 drain source voltage V_{Q3} and the voltage V_{s1} from top to bottom when the snubber circuit is active. At Q_3 turn-off, the diode D_{s1} is forward biased and input current linearly charges the capacitor C_{s1}. The mosfet drain voltage linearly increases till it reaches the output voltage reflected to the transformer primary while V_{s1} stays at *E*. Then the transformer leakage inductance resonates with C_{s1} so that the drain voltage overshoot is controlled by the characteristic impedance and the current in L_1. At Q_3 turn-on, the diode D_{sr1} is forward biased to provide the resonant loop for L_{sr} and C_{s1} till the voltage across V_{Cs1} reaches *-E*. In this stage, V_{s1} is the voltage across the inductor L_{sr}. Finally, the diode D_{s1} conducts, allowing the current in the snubber inductor to return to *E*.

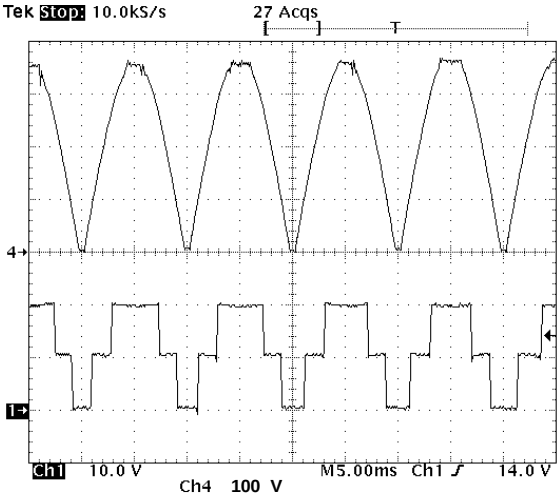

Figure 8. Sinusoidal Modulation Waveforms

6. CONCLUSIONS

In this paper, a current fed two-inductor boost converter topology is proposed. The buck conversion stage allows the DC-DC boost stage to produce rectified sinusoidal voltages, which eases the design of the DC-AC inversion stage to an unfolding stage. Significant efforts have been made in reducing the power loss by using the technologies such as the multiphase converter, the synchronous rectifier, the non-dissipative snubber and the SiC Schottky diodes. A comprehensive set of experimental results is provided. The measurement shows an input power of 57 W and an output power of 51.4 W and this confirms that more than 90% efficiency can be easily achieved for the converter. However, a thorough study on the power loss components in the converter is needed in order to further increase the overall efficiency.

7. REFERENCES

[1] M. Calais, J. Myrzik, T. Spooner and V. G. Agelidis, "Inverters for Single-Phase Grid Connected Photovoltaic Systems – An Overview," *Proc. IEEE PESC, 2002*, pp. 1995-2000.

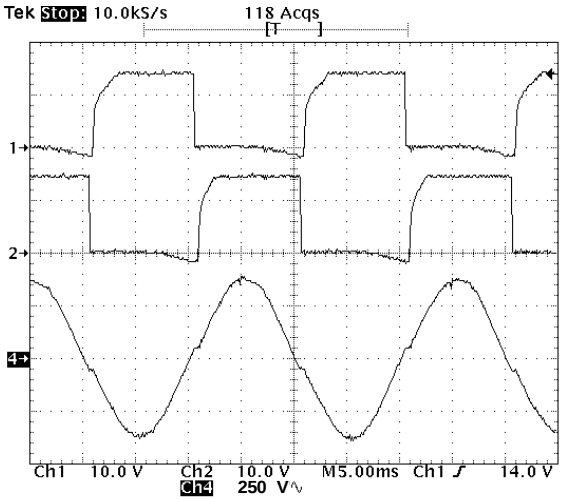

Figure 9. Low Frequency Unfolder Waveforms

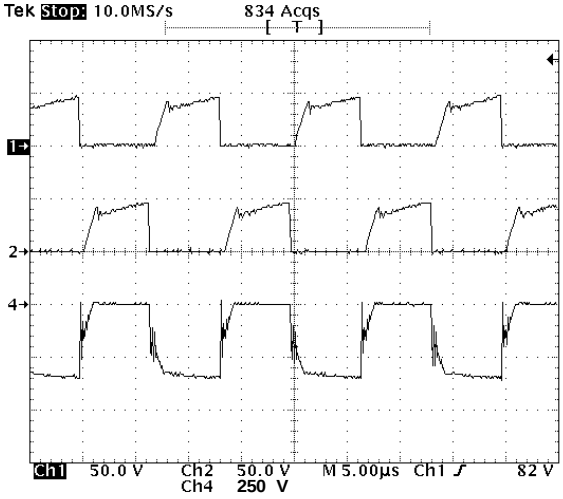

Figure 10. Two-Inductor Boost Converter Waveforms

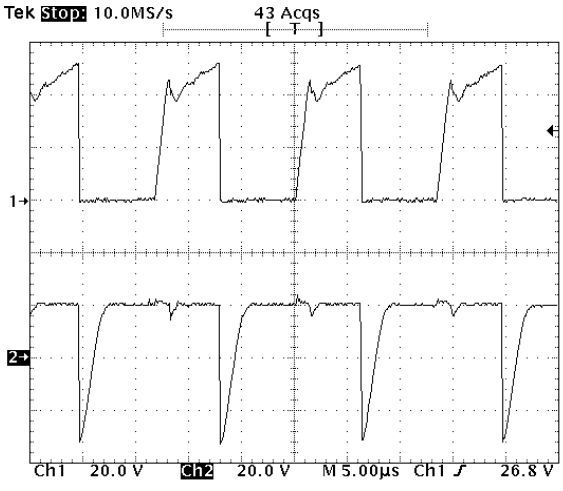

Figure 11. Snubber Waveforms

[2] Q. Li, "Development of High Frequency Power Conversion Technologies for Grid Interactive PV Systems," *Master of Engineering Dissertation*, Central Queensland University, Australia, 2002.

[3] X. Zhou, P. L. Wong, P. Xu, F. C. Lee and A. Q. Huang, "Investigation of candidate VRM topologies for future microprocessors," *IEEE Trans. on Power Electronics*, Vol. 15, No. 6, pp. 1172-1182, Nov. 2000.

[4] W. Chen, "High Efficiency, High Density, Polyphase converters for High Current Applications," *Linear Technology Corporation, 1999*, pp. AN77-1-AN77-16.

[5] Y. Singh and M. J. Kumar, "Lateral Thin-Film Schottky (LTFS) Rectifier on SOI: a Device with Higher than Plane Parallel Breakdown Voltage," *IEEE Trans. on Electron Devices*, Vol. 49, No. 1, pp. 181-184, Jan. 2002.

[6] B. Travis, "The Quest for High Efficiency in Low-Voltage Supplies," EDN, pp. 56-66, 1 September, 2000.

[7] C. Blake, D. Kinzer and P. Wood, "Synchronous Rectifiers versus Schottky Diodes: a Comparison of the Losses of a Synchronous Rectifier versus the Losses of a Schottky Diode Rectifier," *Proc. IEEE APEC, 1994*, pp. 17-23.

[8] B. R. Pelly, *Thyristor Phase-Controlled Converters and Cycloconverters*. New York: John Wiley & Sons, 1971.

[9] F. P. Dawson, "DC-DC Converter Interphase Transformer Design Considerations: Volt-Seconds Balancing," *Digests of International Magnetics Conference, 1990*, pp. ER-05; also in *IEEE Trans. on Magnetics*, Vol. 26, No. 5, pp. 2250 – 2252, Sept. 1990.

[10] G. Bloom and R. Severns, "The Generalized Use of Integrated Magnetics and Zero-Ripple Techniques in Switchmode Power Converters," *Proc. IEEE PESC, 1984*, pp. 15-33.

[11] Q. Li, P. Wolfs, S. Senini, "The Application of the Half Bridge Dual Converter to Photovoltaic Applications", *Proc. AUPEC, 2000*, pp. 156-161.

[12] J. D. Van Wyk and J. A. Ferreira, "Transistor Inverter Design Optimization in the Frequency Range above 5 kHz up to 50 kVA," *IEEE Trans. on Industry Applications*, Vol. IA-19, No. 2, pp. 296-302, March/April 1983.

[13] P. J. Wolfs, "A Current-Sourced DC-DC Converter Derived via the Duality Principle from the Half-Bridge Converter," *IEEE Trans. on Industrial Electronics*, Vol. 40, No. 1, pp. 139-144, Feb. 1993.

[14] M. E. Levinshtein, T. T. Mnatsakanov, P. A. Ivanov, J. W. Palmour, S. L. Rumyantsev, R. Singh and S. N. Yurkov, "High Voltage SIC Diodes with Small Recovery Time," *Electronics Letters*, Vol. 36, No. 14, pp. 1241-1242, Jul. 2000.